JOURNAL OF CATALYSIS 86, 158–172 (1984)

Application of Transient Response Techniques for Quantitative Determination of Adsorbed Carbon Monoxide and Carbon Present on the Surface of a Ruthenium Catalyst during Fischer–Tropsch Synthesis

PHILIP WINSLOW AND ALEXIS T. BELL

Materials and Molecular Research Division, Lawrence Berkeley Laboratory and Department of Chemical Engineering, University of California, Berkeley, California 94720

Received June 25, 1983; revised September 13, 1983

Transient response experiments using isotopic tracers have been carried out to determine quantitatively the coverages of adsorbed CO and carbon on a Ru/SiO_2 catalyst during Fischer–Tropsch synthesis. *In situ* infrared spectra reveal that the Ru surface is virtually saturated by chemisorbed CO. The rate of exchange of adsorbed and gas-phase CO is very rapid compared to the steady-state rate of CO hydrogenation. The integrated absorption coefficient for adsorbed CO is found to decrease from 9.0×10^7 to 4.5×10^7 cm/mol as θ_{CO} increases from 0 to 1.0. Two forms of carbon, C_α and C_β, are also present on the catalyst surface under normal reaction conditions, neither of which is associated with oxygen or hydrogen. C_α is much more reactive than C_β. The surface coverage of C_α rapidly comes to a steady-state value and the steady-state rate of methane formation is found to be a linear function of the C_α coverage. The coverage of C_β is considerably larger than that of C_α and continues to grow over a period of up to 5 min under reaction conditions. C_β is formed from C_α in the presence of adsorbed hydrogen and can be converted back to C_α. It is concluded that at least a part of the C_β deposited resides on the support and that the rest is present on the surface of Ru, and may be responsible for the gradual loss of methanation activity with time. The dependencies of the coverages of C_α and C_β on the partial pressures of the reactants have been determined and are found to be quite different from one another.

INTRODUCTION

Transient response studies, and in particular those involving isotopic tracers, can provide a considerable amount of information regarding the mechanism of Fischer–Tropsch synthesis of hydrocarbons over Group VIII metals. Working with a fused iron catalyst, Bennett and co-workers (*1*, *2*) have observed that upon changing from a flow of CO and H_2 to a flow of H_2 alone, a surface intermediate formed during steady-state synthesis undergoes rapid hydrogenation to produce methane and higher hydrocarbons. The reactivity of this intermediate gradually diminishes when it is annealed in helium, and XPS observations indicate that the intermediate is converted to graphitic carbon. It was also noted that a freshly reduced iron catalyst is progressively carburized under synthesis conditions. Based on this evidence, it was concluded that adsorbed CO rapidly dissociates to form atomic carbon which then acts as a precursor to the synthesis of hydrocarbons, as well as carburization of the catalyst. Using similar experimental techniques, Ekerdt and Bell (*3*) have established that large amounts of carbon are laid down during synthesis over a Ru/SiO_2 catalyst. Here too, it was observed that the carbonaceous deposit could be hydrogenated at a rate considerably in excess of steady-state synthesis rates. Integration of the amounts of methane and C_2^+ hydrocarbons formed during the transient indicated that the carbon reservoir is equivalent to several monolayers of the exposed Ru. Since *in situ* infrared spectra of adsorbed CO showed no attenuation of the CO band intensity during the

0021-9517/84 $3.00

time that the catalyst was under synthesis conditions, it was proposed that the deposited carbon must be located on the support or exist as fine carbon whiskers attached to the surface of the metal

The participation of atomic carbon in the formation of methane and higher molecular weight hydrocarbon over Ni, Co, and Ru catalysts has been demonstrated very effectively by Biloen *et al* (*4*) using transient isotopic tracer techniques In these experiments, the catalyst surface was partially covered by ^{13}C-labeled carbon produced by disproportionating $^{13}C^{16}O$ The undissociated $^{13}C^{16}O$ was then displaced by $^{12}C^{16}O$ and the catalyst was exposed to a mixture of $^{12}C^{16}O$ and H_2 These experiments showed that the ^{13}C-labeled carbon is readily incorporated into the hydrocarbon products and that the dissociation of $^{12}C^{16}O$ is a rapid process By using $^{12}C^{18}O$ to displace the $^{13}C^{16}O$ adsorbed during the Boudouard reaction, Biloen *et al* (*4*) were able to establish that the displacement process is not accompanied by extensive isotopic scrambling, which suggests that CO dissociation is undirectional

Cant and Bell (*5*) combined transient response isotopic tracing with in situ infrared spectroscopy to investigate the dynamics of several elementary processes occurring during CO hydrogenation over a Ru/SiO_2 catalyst Chemisorbed CO was found to exchange very rapidly with gas-phase CO, and under reaction conditions, the two species were established to be in equilibrium A similar conclusion was reached concerning the relationship between gas phase and adsorbed H_2 The dissociation of molecularly adsorbed CO was found to require vacant surface sites While isotopic scrambling between $^{13}C^{16}O$ and $^{12}C^{18}O$ was observed, the rate of this reaction was found to be small compared to the conversion of CO to methane Two interpretations were given for this observation The first is that CO dissociation is nearly irreversible The second is that dissociation is in fact reversible, but isotopic scrambling is impeded by the low mobility of adsorbed carbon and oxygen atoms Experiments similar to those described by Cant and Bell (*5*) have also been reported by Tamaru and co-workers (*6, 7*) These authors concluded that all hydrocarbon species are formed from surface carbon produced by dissociative adsorption of CO Additional carbon was found to be accumulated in the form of hydrocarbon chains It was proposed that these species can resupply the catalyst surface with single carbon atom species by scission of the carbon–carbon bonds in the chains

Biloen *et al* (*8*) have recently performed additional transient response experiments with Ni, Co, and Ru catalysts The results of these studies led them to conclude that only a small fraction of the total carbon overlayer belongs to the reaction intermediates, but that these species are linked to the total carbon reservoir in a reversible fashion A similar picture has been proposed by Happel *et al* (*9–11*) to explain the course of transient responses observed with Ni catalysts From a simulation of the observed transients, these authors deduced that the most abundant reacting intermediate is adsorbed CH, and that the carbidic carbon consists of a relatively small pool of active carbon which exchanges with a larger pool of inactive carbon

The studies presented here represent an extensioin of the work reported by Cant and Bell (*5*) and were aimed at obtaining quantitative measurements of the different forms of carbon present on the surface of a silica-supported Ru catalyst A further objective was to identify the active form of carbon directly involved in the synthesis of methane and higher molecular weight products The influence of reaction conditions on the surface coverages of adsorbed CO and carbon were also examined These investigations were carried out using transient isotopic tracing in combination with Fourier-transform infrared spectroscopy

EXPERIMENTAL

The experimental apparatus used for

these studies is similar to that described by Cant and Bell (*5*) The central component is a low dead-volume reactor that doubles as an infrared cell (*12*) The catalyst, in the form of a 20-mm-diameter pressed disk is held in an aluminum holder between two CaF_2 windows The path length through the gas in the cell is 2 5 mm, and the residence time of the gas in the cell is of the order of 0 25 s The cell is heated by external flat-plate heaters The temperature of the catalyst is measured by a thermocouple, the tip of which is inserted into the catalyst disk holder

Gas for the reactor is supplied from a manifold made up of two branches Up to four separate gases can be delivered to each branch by electronic flow controllers (Precision Flow Devices Model PFD-112) The two branches are connected to a low dead-volume 4-way valve that is used to select the feed stream delivered to the reactor Since the pressure drop in each of the branches is negligible, switching from one stream to the other is accomplished without generation of a pressure surge or changes in gas flow rate Operation of the valve is achieved through a motor-driven valve actuator (Valco 4200)

A portion of the product stream is sampled through a differentially pumped inlet system into a vacuum chamber containing the quadrupole structure and detector of an EAI 250B mass spectrometer (*13*) Selection of the mass spectrometer settings and data acquisition are accomplished using a Commodore PET microcomputer (Model 8032) This system is also used to control the valve actuator and to carry out data analysis after an experiment Under normal operation, the intensities of five separate masses are scanned every 0 33 s and stored on a floppy disk Upon completion of an experiment, the stored data can be displayed on the visible memory of the microcomputer and then plotted on an x–y recorder

Infrared spectra are collected using a Digilab FTS-10M Fourier-transform infrared spectrometer equipped with a narrow-band HgCdTe detector The spectrometer is operated by a Nova 2 computer interfaced to a Data General 6050 5M byte hard disk Using a Real-Time Disk Operating Systems (RDOS), 8-cm^{-1}-resolution spectra were collected in the form of interferograms at the rate of about one per second For archival storage, the spectral data were transferred to magnetic tape An optoelectronic link between the NOVA 2 and the PET was used to synchronize data acquisition by the two computers

A 4 3% Ru/SiO_2 catalyst was prepared by incipient wetness impregnation of Cab-O-Sil HS-5 with an aqueous solution of $RuCl_3$ $3H_2O$ The catalyst was dried and reduced in flowing H_2, for 2 h at 673 K The catalyst was then sieved, and 51 mg of the −30, +60 mesh fraction was pressed into a self-supporting disk The dispersion of the catalyst sample was determined to be 0 27, by means of H_2 chemisorption at 373 K

Hydrogen, deuterium, and helium were purified by passage through Oxy-Absorbent (Alltech Associates No 4005) and molecular sieve (Linde 13×) cooled in liquid nitrogen Mass spectrometric analysis of the deuterium indicated a 2 3% content of HD Carbon monoxide was purified of iron carbonyls by passage through a copper tube packed glass beads and heated to 473 K Further purification was accomplished by passage through Ascarite II and molecular sieve cooled in dry ice Isotopically labeled CO was obtained from Liquid Carbonic and used without further purification Mass spectrometric analysis showed that the $^{13}C^{16}O$ contained 3 6% $^{12}C^{16}O$, 0 8% $^{12}C^{18}O$, and 11 8% $^{13}C^{18}O$, and that the $^{12}C^{18}O$ contained 0 9% $^{12}C^{16}O$ and 0 9% $^{13}C^{18}O$

RESULTS

Steady-State Kinetics

The steady-state kinetics of methane synthesis were determined using $^{13}C^{16}O$ and D_2 as the reactants The choice of reactants was dictated by the fact that both $^{13}C^{16}O$

and D_2 were used in the isotopic tracer experiments aimed at determining the surface coverages of adsorbed CO and carbon By using D_2, rather than H_2, it was also possible to determine the production of ^{13}C-labeled methane by monitoring mass 21, without interference from the fragmentation patterns for water and other methane isotopes Rate measurements were made for temperatures between 443 and 513 K, CO partial pressures between 59 and 195 Torr, and D_2 partial pressures between 88 and 588 Torr Prior to each measurement the catalyst was reduced in flowing D_2 for 24 h at 463 K

For the sake of consistency, the rate data used to establish the kinetics of $^{13}CD_4$ synthesis were all collected after 300 s of reaction These data are well represented by the expression

$$N_{C_1} = 4.2 \times 10^8 \frac{P_{D_2}^{1.23}}{P_{CO}^{0.86}} \exp(-25{,}300/RT) \quad (1)$$

where N_{C_1} is the turnover frequency for $^{13}CD_4$ formation in s^{-1}, P_{D_2} is the partial pressure of D_2 in atm, P_{CO} is the partial pressure of $^{13}C^{16}O$ in atm, and T is the temperature in Kelvin degrees Both the activation energy and the exponents on the partial pressures of D_2 and CO are in good agreement with previous determinations of the kinetics of methane synthesis over silica- and alumina-supported Ru (*3, 6, 14–17*)

In addition to methane, small amounts of ethane and ethylene were observed The rates of formation of these products were usually about 10% of the rate of methane formation Since accurate measurements of the rates of the C_2 species were difficult to make, the kinetics of their formation were not determined

Chemisorbed CO

Infrared spectra of the catalyst taken under reaction conditions exhibited a single band attributable to linearly adsorbed CO At 463 K, neither the position nor the integrated absorbance of this band changed as the partial pressure of CO was varied between 60 and 200 Torr, and the partial pressure of D_2 was varied between 0 and 580 Torr The position of the band did depend, though, on the isotopic composition of the CO The band was observed at 2040 cm^{-1} for $^{12}C^{16}O$, at 1995 cm^{-1} for $^{12}C^{18}O$, and at 1990 cm^{-1} for $^{13}C^{16}O$ Between 433 and 493 K, the CO band was unaffected by the catalyst temperature When the temperature was raised to 513 K, the integrated-band intensity decreased, but only by about 4%

Two independent methods were used to correlate the integrated band intensity with the coverage of adsorbed CO The first involved saturation of the catalyst surface with $^{12}C^{16}O$ followed by a gradual reduction of the adsorbate with D_2 At 463 K, the time constant for CO reduction was approximately 4 min, which is considerably longer than the time constant for diffusion through the catalyst disk, $\ll 1$ s This assures that during the reduction a uniform partial coverage is maintained throughout the disk By measuring the amount of $^{12}C^{16}O$ removed as $^{12}CD_4$ and a knowledge of the total amount of adsorbed $^{12}C^{16}O$ present at the start of the experiment, it is possible to determine the amount of $^{12}C^{16}O$ remaining on the catalyst surface at any time This quantity can then be correlated with the integrated absorbance of the CO band

The second method involved a direct determination of the coverage by adsorbed CO The catalyst was first saturated with $^{12}C^{18}O$ A partial coverage was then achieved by reducing a portion of the adsorbate in a manner identical to that described above The reactor was then flushed with argon for 60 s and the spectrum of the remaining adsorbate was recorded Next, a flow of 5% $^{13}C^{16}O$ was introduced into the reactor This caused the adsorbed $^{12}C^{18}O$ to be rapidly displaced by $^{13}C^{16}O$ and produced a well-defined transient of $^{12}C^{18}O$ in the gas phase The integral of this transient is equivalent to the quantity of originally adsorbed $^{12}C^{18}O$ Experi-

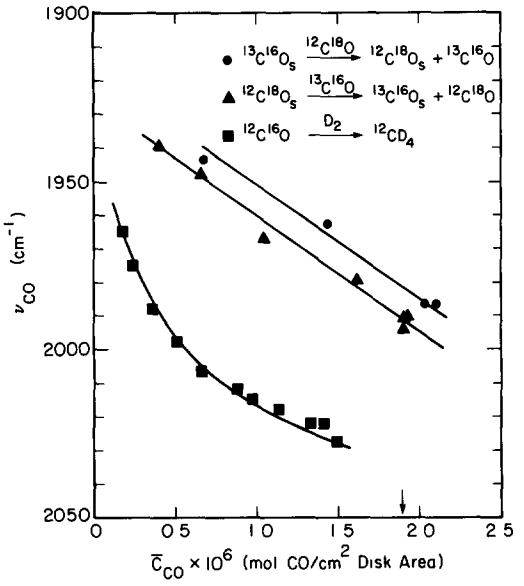

FIG 1 Effect of the concentration of adsorbed CO on ν_{CO} The arrow indicates the concentration corresponding to CO/Ru$_s$ = 1 0

ments, similar to those just described, were also carried out in which the catalyst was first contacted with $^{13}C^{16}O$ and the adsorbed $^{13}C^{16}O$ then displaced with $^{12}C^{18}O$ No evidence was found during this experiment for the formation of $^{13}C^{18}O$ or $^{12}C^{16}O$

Figures 1 and 2 illustrates the effects of CO surface coverage on the vibrational frequency, integrated absorbance, and the integrated absorption coefficient The data given in Fig 1 show that the vibrational frequency, ν_{CO}, decreases progressively with decreasing surface coverage This trend has been observed in many infrared studies of adsorbed CO and is ascribable to a decrease in dipolar coupling (*18*) The dependence of the integrated absorbance on adsorbate coverage, seen in Fig 2A, is identical for all three forms of CO and is independent of the method used to determine the surface coverage At low coverages, the integrated absorbance increases linearly with coverage, but at higher coverages the integrated absorbance increases more slowly The integrated absorption coefficient, $\bar{A}_{CO}$, was determined from the expression

$$\bar{A}_{CO} = \frac{1}{\bar{C}_{CO}} \int_{1500}^{2100} A(\nu) d\nu$$

As can be seen in Fig 2B, $\bar{A}_{CO}$ decreases with increasing surface coverage The magnitude of $\bar{A}_{CO}$ for CO adsorbed on Ru/SiO$_2$ is similar to that reported previously for CO adsorbed on Pt/SiO$_2$ (*18–23*), as indicated by the data given in Table 1 It is also of interest to note that the decline in $\bar{A}_{CO}$ with increasing CO coverage is similar in extent

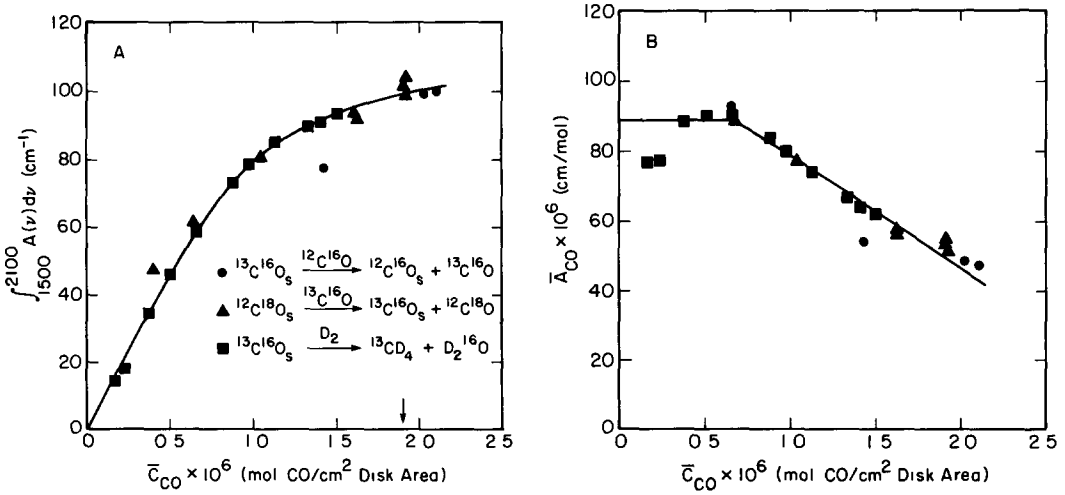

FIG 2 Effect of the concentration of adsorbed CO on (*a*) the integrated absorbance of the CO band and (*b*) the integrated absorption coefficient The arrow indicates the concentration corresponding to CO/Ru$_s$ = 1 0

TABLE 1

Comparison of Integrated Absorption Coefficients for CO Adsorbed on Ru and Pt

Source	Catalyst	$\bar{A}_{CO} \times 10^{-6}$ (cm/mol)
This work	Ru/SiO_2	90–45[a]
Heyne and Tompkins (*19*)	Pt/SiO_2	55–30[a]
Eischens (*20*)	Pt/SiO_2	73–40[a]
Seanor and Amberg (*21*)	Pt/SiO_2	37,29[b]
Cant and Donaldson (*22*)	Pt/SiO_2	43,51[b]

[a] The range in $\bar{A}_{CO}$ values reflects the change observed with increasing CO coverage

[b] Values of $\bar{A}_{CO}$ obtained at saturation coverage with two catalyst samples

to that reported for silica-supported Pt (*18–23*) and for Ru(001), Pt(111), and Pt(100) surfaces (*24–26*)

Chemisorbed Carbon

The following procedure was used to determine the quantity of carbon present on the catalyst surface The catalyst was first reduced at 463 K and then exposed to a $^{13}C^{16}O/D_2$ mixture for a period of 15 to 300 s Following steady-state operation of the catalyst for the desired period of time, the feed to the reactor was switched from the $^{13}C^{16}O/D_2$ mixture to a $^{12}C^{16}O/D_2$ mixture of equivalent composition Figure 3 shows a series of infrared spectra taken immediately after the switch in isotopic composition of the feed The position of the CO band is seen to shift to higher frequencies as $^{12}C^{16}O$ displaces the adsorbed $^{13}C^{16}O$ The displacement process is very rapid and is over in about 4–5 s A plot of the gas-phase concentration of $^{13}CD_4$ during isotopic displacement is illustrated in Fig 4 It is seen that while the rate of $^{13}CD_4$ formation undergoes a decline upon substitution of $^{12}C^{16}O$ for $^{13}C^{16}O$, the time constant for this process is significantly longer than that for the displacement of adsorbed CO and, in fact, measurable rates of $^{13}CD_4$ formation could be observed for up to 600 s following the substitution of CO isotopes This indicates that a reservoir of ^{13}C remains on the

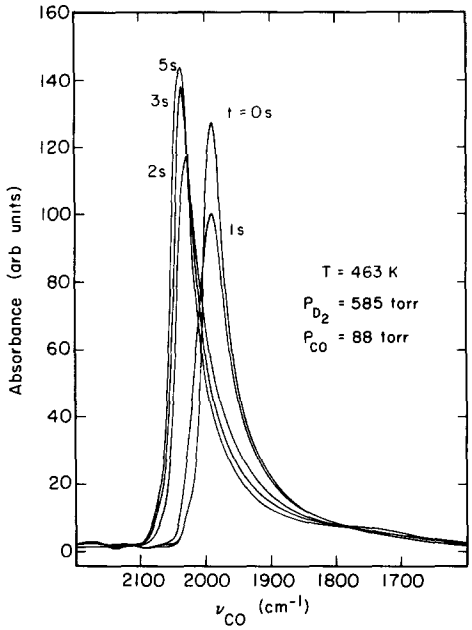

FIG 3 Infrared spectra of adsorbed CO illustrating the displacement of $^{13}C^{16}O$ by $^{12}C^{18}O$ under steady-state reaction conditions

surface long after all of the adsorbed $^{13}C^{16}O$ has been displaced The amount of ^{13}C removed from the catalyst as $^{13}CD_4$ during this period will be referred to as reactive carbon, C_r

After a fixed period of exposure of the catalyst to the $D_2/^{12}C^{16}O$ mixture, the reactor was flushed with helium for 0–120 s D_2 was then introduced to react off all residual carbon-containing species Figure 4 shows that upon introduction of D_2, a rapid rise occurs in the formation $^{13}CD_4$ which

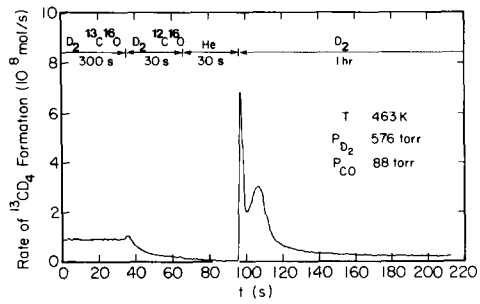

FIG 4 The rate of $^{13}CD_4$ formation during the sequence $D_2/^{13}C^{16}O$ (300 s) → $D_2/^{12}C^{16}O$ (30 s) → He (30s) → D_2 (3600 s) Total flow rate = 1 42 STP cm^3/s

reaches a maximum after about 2 s This sharp peak is then followed by a broader peak occurring between 10 and 60 s The two peaks are attributed to different forms of carbon designated as C_α and C_β The amount of C_α is defined by the carbon removed during the first 5 s of titration by D_2, and the amount of C_β as the amount of carbon removed after 5 s of titration The absence of significant quantities of deuterium in association with either C_α or C_β is suggested by H_2/D_2 tracer experiments conducted with Ru-black Additional support for this conclusion can be drawn from recent solid-state ^{13}C NMR studies (*26*), which show no evidence for C—H or C—D coupling on the spectra of C_α and C_β present on Ru/SiO_2

Due to complications arising from overlapping cracking patterns, the transients in $^{12}CD_4$ were not observed during the course of the experiment presented in Fig 4 These data were obtained, though, by reversing the sequence of introduction of the $^{13}C^{16}O/D_2$ and $^{12}C^{16}O/D_2$ mixtures, and observing the transients in $^{13}CD_4$ The results are presented in Fig 5 In this case, there is no production of $^{13}CD_4$ during the first phase of the experiment while $^{12}C^{16}O$ and D_2 are being fed to the reactor Upon introduction of the $^{13}C^{16}O/D_2$ mixture, $^{13}CD_4$ begins to form and the rate of production of this product steadily increases Comparison of Figs 4 and 5 shows that the methane transients for this part of the experiment

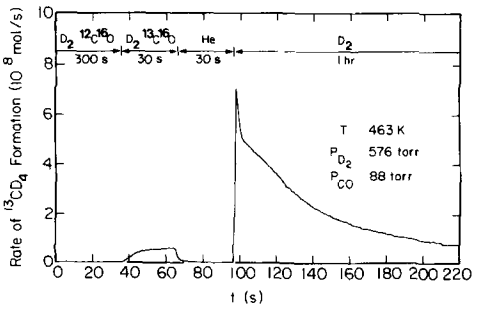

FIG 5 The rate of $^{13}CD_4$ formation during the sequence $D_2/^{12}C^{16}O$ (300 s) → $D_2/^{13}C^{16}O$ (30 s) → He (30 s) → D_2 (3600 s) Total flow rate = 1 42 STP cm³/s

have a complementary relationship The methane transient observed during the final phase of the experiment shown in Fig 5 is quite different from that shown in Fig 4 The sharp peak seen at the beginning of the response is due to the reduction of a small amount of ^{13}C-labeled C_α, produced during the period following the introduction of the $^{13}C^{16}O/D_2$ mixture The broader transient comprising the bulk of the response is due to the reduction of adsorbed CO Infrared spectra taken as a function of time show that the decrease in the absorbance of the $^{13}C^{16}O$ band exactly parallels the production of $^{13}CD_4$

To ascertain whether the α and β forms of carbon are associated with any oxygen, an experiment similar to that shown in Fig 4 was performed using a $^{12}C^{18}O/D_2$ in the first step of the sequence If either C_α or C_β was bonded to oxygen, then it would be expected that a transient in $D_2{}^{18}O$ would be observed during the reaction of the catalyst with D_2 Since such transients were not observed, it is concluded that neither C_α or C_β is associated with oxygen

A series of experiments was conducted in which the steady-state reaction time was varied from 15 to 300 s, to determine the influence of reaction time on the surface concentration of C_α and C_β In each of these experiments, the duration of CO isotopic exchange was kept constant at 30 s and the duration of the helium flush was held to 15 s It was observed that the rate of methane synthesis slowly declined from $2\ 9 \times 10^{-3}$ to $2\ 6 \times 10^{-3}$ s^{-1} as the reaction time increased from 15 to 300 s Over the same period of time, the integrated absorbance of the CO band remained constant to within ±1% Figure 6 shows the transients in $^{13}CD_4$ observed during the reduction of elemental carbon present on the catalyst surface The amounts of C_α and C_β, determined by integration of the peaks presented in Fig 6, are shown in Fig 7, as functions of the steady-state reaction time Also shown in this figure is the amount of reactive carbon removed during the 30 s follow-

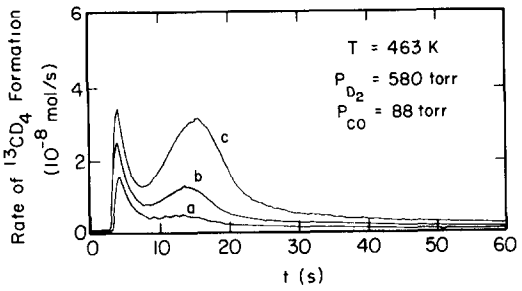

FIG 6 Effect of the length of time under reaction conditions on the transient in $^{13}CD_4$ formation observed during reduction of the catalyst with D_2 The gas introduction sequence is the same as that used for the experiment shown in Fig 4 Duration of reaction in $D_2/^{13}C^{16}O$ (a) 10 s, (b) 60 s, (c) 300 s Duration of exposure to $D_2/^{12}C^{16}O$ 30 s Duration of He flush 15 s Total flow rate 1 42 STP cm^3/s

ing the substitution of $^{12}C^{16}O$ for $^{13}C^{16}O$ The amounts of C_r and C_α increase rapidly during the first 60 s of steady-state reaction and then remain fairly constant thereafter The close parallel in the temporal behavior of C_r and C_α strongly suggests that these are equivalent forms of carbon The plateau in the total amount of C_r plus C_α corresponds to 0 02 of a Ru monolayer The amount of C_β increases monotonically with steady-state reaction time and reaches a level corresponding to 0 13 of a Ru monolayer after 300 s of reaction

A separate series of experiments was carried out to determine the influence of the rates at which C_α and C_β are removed from the catalyst surface during the period of exposure to $^{12}C^{16}O$ For these experiments, the reaction time was held constant at 300 s while the duration of exposure to $^{12}C^{16}O$ was varied from 15 to 600 s A helium flush time of 15 s was used in all cases The transient responses for $^{13}CD_4$ are shown in Fig 8, and plots of the amounts of C_α, C_r, and C_β versus $^{12}C^{16}O$ exposure time are shown in Fig 9 It is apparent from both figures that as the exposure time to $^{12}C^{16}O$ increases, the reservoir of C_α decreases much more rapidly than the reservoir of C_β The integral of the $^{13}CD_4$ produced during exchange with $^{12}C^{16}O$ corresponds to the amount of carbon removed from the surface as C_r Figure 9 shows that this amount increases with time of exposure to $^{12}C^{16}O$, but that the sum of the amounts of C_α, C_β, and C_r remains the same It is also interesting to note that for very short $^{12}C^{16}O$ exposure times (<30 s), $d\theta_{C_r}/dt \approx -d\theta_{C_\alpha}/dt$, whereas for long $^{12}C^{16}O$ exposure times (>500 s) $d\theta_{C_r}/dt \approx -d\theta_{C_\beta}/dt$

The fact that C_α is more reactive than C_β, and the fact that the reservoir of C_α rapidly comes to a steady-state value with reaction time, strongly suggests that C_α is a primary intermediate in the formation of methane under steady-state conditions If this hypoth-

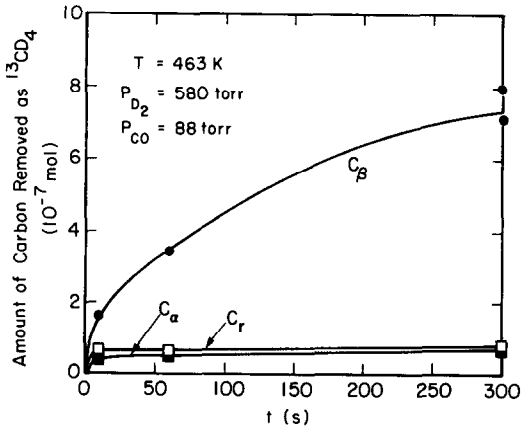

FIG 7 Effect of the length of time under reaction conditions on the amount of C_α, C_β, and C_r

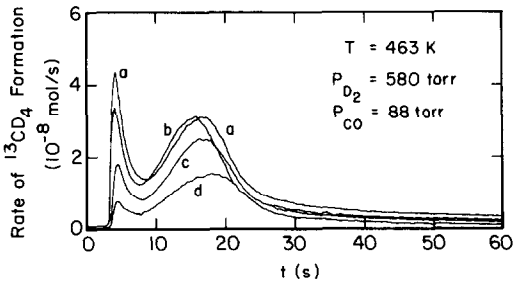

FIG 8 Effect of the duration of exposure to $D_2/^{12}C^{16}O$ on the transient in $^{13}CD_4$ formation observed during the reduction of the catalyst with D_2 The gas introduction sequence is the same as that used for the experiment shown in Fig 4 Duration of reaction in $D_2/^{13}C^{16}O$ 300 s Duration of exposure to $D_2/^{12}C^{16}O$ (a) 15 s, (b) 30 s, (c) 120 s, (d) 600 s Duration of He flush 15 s Total flow rate 1 42 STP cm^3/s

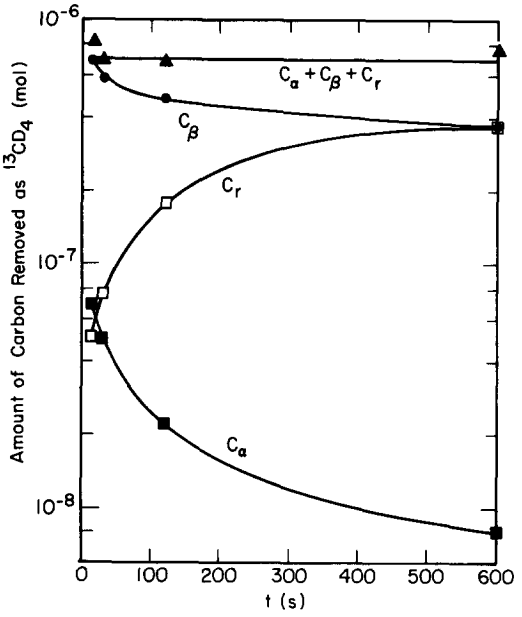

FIG 9 Effect of the duration of exposure to D_2/$^{12}C^{16}O$ on the content of ^{13}C in the reservoirs of C_α, C_β, and C_r The results shown here are based on the data presented in Fig 8

esis is correct, then the rate of methanation should be proportional to the amount of C_α on the catalyst surface Figure 10 illustrates a plot of the rate of $^{13}CD_4$ formation versus the amount of $^{13}C_\alpha$ The four filled points were obtained from data taken during the period following the substitution of $^{13}C^{16}O$ by $^{12}C^{16}O$ It is apparent that these points lie along a straight line which passes through the origin of the plot

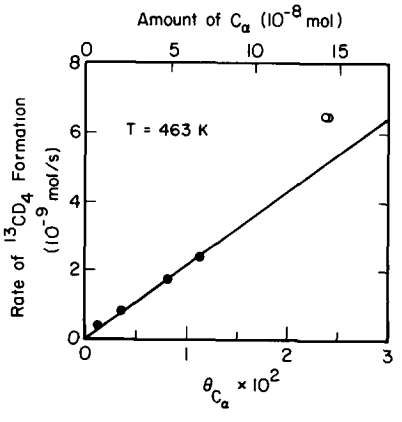

FIG 10 Dependence of the rate of $^{13}CD_4$ formation on θ_{C_α}

If Fig 10 properly describes the relationship between the methanation rate and the reservoir of C_α, the value of the abscissa for the point corresponding to the steady-state methanation rate (following 300 s of reaction) should correspond to the total amount of C_α present on the surface under steady-state conditions The amount of C_α determined in this manner is $1\ 85 \times 10^{-7}$ mol This figure compares favorably with $1\ 47 \times 10^{-7}$ mol, the estimate of C_α present under steady-state conditions, obtained from Fig 4

The relationship of C_α and C_β to one another was investigated through a separate set of experiments In the first, the catalyst was exposed initially to a flow of helium containing 87 Torr of $^{13}C^{16}O$, for 300 s at 463 K The $^{13}C^{16}O$ was then replaced by $^{12}C^{16}O$, to displace the adsorbed $^{13}C^{16}O$ Following a 15-s flush in helium, the residual ^{13}C was removed by reaction with D_2 Figure 11 shows that only a single peak of $^{13}CD_4$ was observed in this experiment The position, magnitude, and shape of the peak corresponded very closely to those for the C_α peak seen normally This result strongly suggests that in the absence of D_2, CO dissociates to produce C_α alone

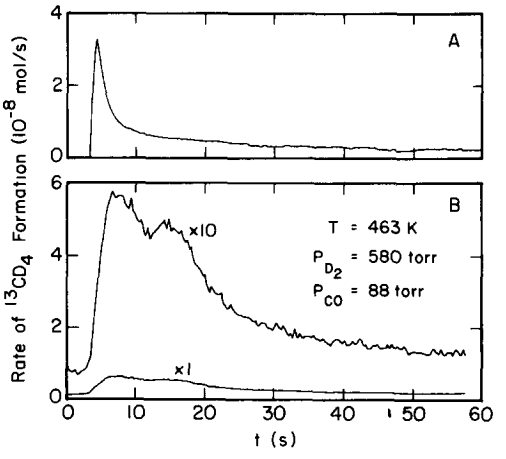

FIG 11 Transients in $^{13}CD_4$ formation observed during reduction of the catalyst in D_2 The gas introduction sequence for these experiments is (A) $^{13}C^{16}O$ (300 s) → $^{12}C^{16}O$ (30 s) → He (15 s) → D_2 (3600 s), (b) $^{13}C^{16}O$ (300 s) → D_2/$^{12}C^{16}O$ → D_2 (3600 s)

In a second experiment, the catalyst, was again exposed for 300 s to a gas mixture containing $^{13}C^{16}O$ This time, though, the isotopic displacement of adsorbed CO was carried out using a mixture containing $^{12}C^{16}O$ and D_2 As can be seen in Fig 11, subsequent titration of the surface with D_2 produced a transient response for $^{13}CD_4$, which had two peaks The second of these was similar in position and shape to the peak normally observed for C_β This experiment suggests that C_α can readily be converted into C_β but that this process requires the presence of D_2

The conversion of C_α into C_β can be reversed, as demonstrated by the results presented in Fig 12 In this instance a normal gas delivery sequence was used, with the exception that the period of helium flushing was increased from 15 to 120 s The data show that, as the duration of helium flushing increases, the C_β peak decreases and the C_α peak increases

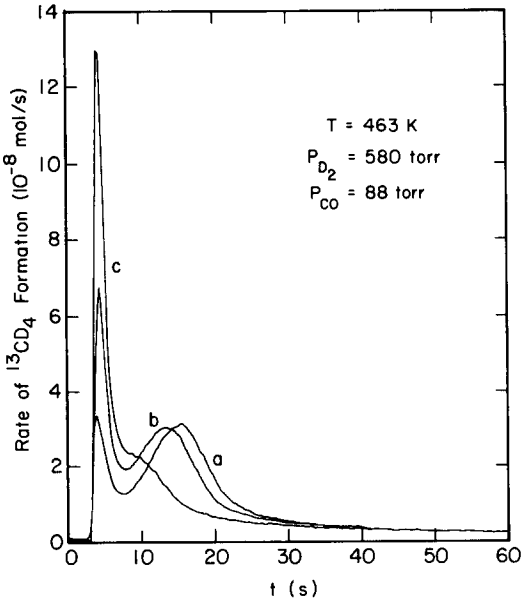

FIG 12 Effect of the duration of He flushing on the transient in $^{13}CD_4$ formation during the reduction of the catalyst with D_2 The gas introduction sequence is the same as that used for the experiment shown in Fig 4 Duration of reaction in $D_2/^{13}C^{16}O$ 300 s Duration of exposure to $D_2/^{12}C^{16}O$ 30 s Duration of He flush (a) 15 s, (b) 30 s, (c) 120 s Total flow rate 1 42 STP cm^3/s

The influence of reaction conditions on the coverages of the catalyst by C_α and C_β were investigated by varying the temperature and the partial pressures of $^{13}C^{16}O$ and D_2 during the period of steady-state reaction At 463 K, and for $^{13}C^{16}O$ and D_2 partial pressures between 59 and 195 Torr and 177 and 580 Torr, respectively, the coverages by C_α and C_β are correlated by the following expressions

$$\theta_{C_\alpha} = 4\,4 \times 10^{-3}\,(P_{D_2}/P_{CO})^{0\,83} \quad (2)$$

$$\theta_{C_\beta} = 1\,3\,P_{D_2}^{0\,14}\,P_{CO}^{0\,77} \quad (3)$$

where P_{D_2} and P_{CO} are in atmospheres It is to be noted that while the coverage by C_α depends only on the D_2/CO ratio, the coverage by C_β increases with the partial pressures of both reactants

The effects of temperature on the coverages by C_α and C_β are illustrated in Figs 13 and 14 Figure 13 shows that as the temperature increases from 443 to 513 K, the peak attributed to the reduction of C_β rapidly shifts to earlier times and merges with the peak for the reduction of C_α Above 473 K, resolution of the transient into two separate peaks is no longer possible The change in the position of the two peaks with temperature indicates that the process leading to

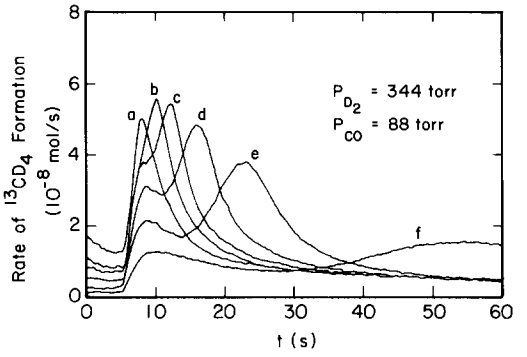

FIG 13 Effect of temperature on the transient in $^{13}CD_4$ formation observed during the reduction of the catalyst with D_2 The gas introduction sequence is the same as that used for the experiment shown in Fig 4 Temperature (a) 513 K, (b) 493 K, (c) 483 K, (d) 473 K, (e) 463 K, (f) 443 K Duration of reaction in $D_2/^{13}C^{16}O$ 300 s Duration of He flush 15 s Total flow rate 1 42 STP cm^3/s

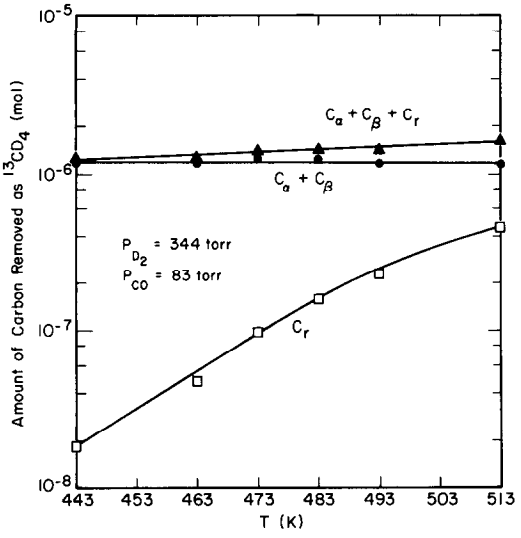

FIG 14 Effect of temperature on the amounts of C_α, C_β, and C_r

the removal of C_β are significantly more sensitive to temperature than the processes involved in the removal of C_α The effect of temperature on the total amount of C_α and C_β removed from the surface after 5 min of reduction is shown in Fig 14 Also shown is the amount of C_r removed during the 30 s that the catalyst is exposed to $^{12}C^{16}O$

It is apparent that the amount of carbon removed as C_r increases rapidly with temperature, but that the total amount of C_α plus C_β, residual on the catalyst surface prior to reduction by D_2 is nearly independent of temperature These data indicate that the total amount of carbon accumulated on the catalyst surface after 300 s of steady-state operation increases only moderately with temperature A possible reason for the insensitivity of the carbon coverage to temperature may be that the overall activation energies associated with the rates of production and consumption of carbon are comparable

Formation of C_2 Products

The principal hydrocarbons observed in addition to methane were ethylene and ethane While it was not possible to judge the ratio of olefin to paraffin accurately from the mass spectrometric data, studies of the synthesis kinetics over silica- and alumina-supported Ru catalysts performed by Kellner and Bell (*14*) indicate that the ratio should be 4 4 for the conditions used for the major part of this study (T = 463 K, P_{D_2} = 585 Torr, P_{CO} = 88 Torr) For these same conditions, the rate of formation of C_2 products is roughly 10% of the rate of methane formation

Isotopic tracer experiments similar to those illustrated in Fig 3 were carried out in order to define the extent of participation of C_α and C_β in the formation of C_2 hydrocarbons Figure 15 show the mass spectrometer traces observed for masses 34 and 33 The first of these signals corresponds to the most intense peak present in the mass spectra of $^{13}C_2D_4$ and $^{13}C_2D_6$, and the second, to the most intense peaks seen in the mass spectra of $^{13}CD_2{}^{12}CD_2$ and $^{13}CD_3{}^{12}CD_3$ When the $^{13}C^{16}O/D_2$ mixture is fed to the reactor, the intensity of the mass 34 signal is high and intensity of the mass 33 is almost zero The small amount of mixed-labeled C_2 products formed is due to the presence of 3 6% of $^{12}C^{16}O$ as an impurity in the $^{13}C^{16}O$ Upon introduction of the $^{12}C^{16}O/D_2$ mixture, the intensity of the mass 34 signal at first decreases due to the consumption ^{13}C carbon present on the catalyst surface The intensity of this signal passes through a minimum at about 10 s and then begins to increase as more and more $^{12}C_2D_6$

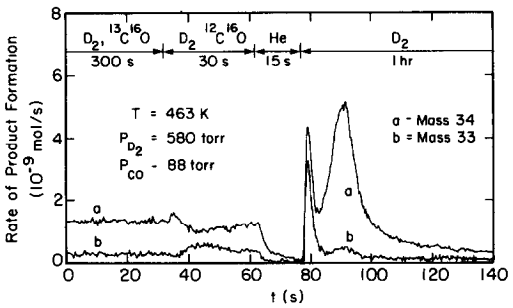

FIG 15 Transients observed in the responses for mass 34 (a) and mass 33 (b) The gas introduction sequence and duration of exposure to each gas are the same as those used for the experiment shown in Fig 4

is formed The mass 33 signal follows a pattern which is the inverse of the mass 34 signal Since the only contribution to mass 33 is from the mixed-labeled C_2 products, the dynamics of the mass 33 signal provide a good indication of the rapidity with which ^{12}C carbon is formed and incorporated into the C_2 products Careful inspection of Figs 4 and 15 shows that the latter process is very rapid, since the rate of increase of the mass 33 signal, during the period of exposure to the $^{12}C^{16}O/D_2$ mixture, is virtually the same as the rate of increase in the signal for the formation of methane from the newly introduced isotope

The transients observed in the mass 34 and 33 signals during the reduction of the adsorbed ^{13}C carbon show two distinct peaks The positions of these peaks are identical to the positions of the methane peaks seen in Fig 3, for the reduction of C_α and C_β The only difference in the mass 34 and 33 signals is in the relative intensities of the C_α and C_β peaks Whereas the C_β peak is quite pronounced for mass 34, it is considerably smaller for mass 33 This latter observation is consistent with the fact that the conversion of C_α to C_β is a relatively slow process, and hence that during the 30 s of exposure of the catalyst to the $^{12}C^{16}O/D_2$ mixture, little of the ^{12}C in the C_α reservoir is transferred to the C_β reservoir

DISCUSSION

The results presented in this paper clearly demonstrate the existence of two forms of carbon on the surface of Ru C_α is produced via the dissociation of adsorbed CO, and as demonstrated by the data presented in Fig 11A, this process does not require the involvement of adsorbed deuterium Under normal reaction conditions, the surface concentration of C_α rapidly achieves a steady-state level and it is observed that the rate of methane synthesis is directly proportional to the surface concentration of C_α The data presented in Fig 11B strongly suggest that C_β is formed from C_α, and that this process requires the participation of adsorbed deuterium As shown in Fig 12, the conversion of C_α to C_β appears to be reversible While not demonstrated by direct experimental evidence, it seems reasonable to suspect that the conversion C_β to C_α also involves the participation of adsorbed hydrogen

The coexistence of two forms of carbon on the catalyst surface is consistent with the proposals recently made by Kobori *et al* (*6*), Biloen *et al* (*8*), and Otarod *et al* (*11*) In each case, the authors have suggested that the form of carbon responsible for the synthesis of methane and C_2^+ hydrocarbons comprises only a small fraction of the total carbon deposit, and that the active form of carbon communicates in a reversible fashion with the reservoir of less active, or inactive, carbon Kobori *et al* (*6*) have proposed, in addition, that the less active form of carbon is present in the form of hydrocarbon chains attached to the surface of the metal This conclusion was based on infrared observations (*7*) of the dynamics of build up and depletion of adsorbed hydrocarbon moieties While the work of Kobori *et al* (*6*) and that reported here both concern Ru, the interpretations differ In the course of this work, no evidence was found for the accumulation of hydrocarbon groups, even though adequate sensitivity was available for the detection of these species by infrared spectroscopy Likewise, ^{13}C NMR studies show no indication of hydrogen attached to the deposited carbon (*26*) This leads to the conclusion that under the conditions of the present experiments, neither the α- or β-forms of carbon are hydrocarbon-like in structure

In the work of Cant and Bell (*5*), experiments similar to those reported here were performed The failure of these authors to observe C_β is very likely due to their choice of reaction conditions As indicated by Eq (3), the coverage by C_β is proportional to the product $P_{CO}^{0.8} P_{H_2}^{0.14}$ The partial pressures of CO and H_2 used by Cant and Bell (*5*) were one-third or less than those used in

the present work This would lead to a much smaller accumulation of C_β in the same time of steady-state operation While no distinct peak for C_β was observed by Cant and Bell (*5*) during the removal of surface carbon with H_2, it is possible that a portion of the tail on the C_α peak which they observed may have, in fact, been due to the reaction of a small amount of C_β

In contrast to the work of Cant and Bell (*5*), Ekerdt and Bell (*3*) observed that the accumulation of carbon following 120 min of synthesis at 464 K over a Ru/SiO_2 catalyst corresponded to several monolayers of Ru Reduction of this reservoir produced not only methane but also ethane and propane The rates at which these products were formed greatly exceeded the steady-state synthesis rates and the production of hydrocarbons continued for over 30 min following the onset hydrocarbon reduction Ekerdt and Bell (*3*) also observed that while the carbon reservoir exceeded several Ru monolayers, its presence did not interfere at all with the chemisorption of CO This led to the conclusion that the carbon resides either on the silica support or is present in the form of thin filaments attached to only a small fraction of the exposed metal surface When viewed in the light of the present results, it seems reasonable to conclude that the form of carbon undergoing reduction in the experiments of Ekerdt and Bell (*3*) was C_β This form of carbon reacts much more slowly than C_α and is present in significantly larger quantities The analogy between the two studies also suggests that most of the C_β observed in this study exists in a form which does not occupy a large fraction of the Ru surface

The relationships between gas-phase CO, adsorbed CO, and the α- and β-forms of surface carbon may be described by the reaction sequence illustrated in Fig 16 With the exception of the pathway shown for the formation of C_β, this sequence is similar to that described in several previous studies (*3, 4, 6, 8, 11, 14*) The very rapid displacement of adsorbed $^{13}C^{16}O$ by gaseous $^{12}C^{16}O$, observed in Fig 3, suggests that under reaction conditions, gas-phase and adsorbed CO are in equilibrium with each other The absence of any isotopic scrambling between carbon and oxygen when adsorbed $^{12}C^{18}O$ is displaced by $^{13}C^{16}O$ suggest that the dissociation of adsorbed CO may be irreversible An alternative explanation is that association does occur but that the surface mobility of C and O atoms is insufficient to achieve homogeneous mixing of these species (*5*) The conversion of C_α to methane is shown to proceed through a partially deuterated species designated as CD_x This symbol is used to represent what is probably a mixture of methyne, methylene, and methyl groups (*27, 28*) Since the degree of coordination of these species to the surface, is expected to be less than that for free carbon atoms, they should be more mobile Several authors (*4, 14, 27, 28*) have suggested that the formation of higher molecular hydrocarbons is initiated by migration of a methyl group to a methylene group to form an ethyl group The rapid appearance of $D_3{}^{12}C^{13}CD_3$ when $^{12}C^{16}O$ is substituted for $^{13}C^{16}O$, shown in Fig 15, is consistent with the postulated mobility of CD_x species If upon coupling the C_2D_5 species were to lose deuterium, it would be easy to see how a carbon dimer might be formed Similar processes can be envisioned to explain the formation of higher oligomers of carbon It is also possible to see how, under appropriate circumstances, such precursors might lead to the formation of graphitic carbon (*29*)

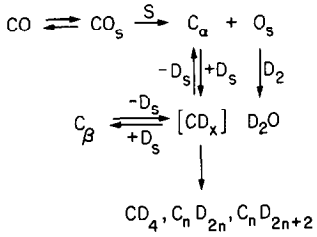

FIG 16 Proposed scheme for the connection of CO_s, C_α, C_β, and CD_x

The location of the C_β relative to the Ru microcrystallites is difficult to establish unambiguously If it is assumed that C_β accumulates on the surface of the microcrystallites in a structure that is one-carbon-atom thick, one would anticipate that the corresponding blockage of Ru sites would lead to an attenuation in the coverage by chemisorbed CO and to a decrease in the rate of methane synthesis As was noted earlier, the accumulation of C_β to a level equivalent to 0 13 of a Ru monolayer does not cause an observable reduction in the integrated absorbance of CO However, this does not necessarily mean that a reduction in CO coverage has not occurred since, as shown in Fig 2A, the curve of integrated absorbance versus CO coverage is nearly flat at high CO coverages There does appear to be a correlation, though, between the rate of methane synthesis and the accumulation of β-carbon In the interval between 60 and 300 s of reaction, the turnover frequency for methane synthesis decreases by about 18% Over the same period, the coverage by C_β increases by about 7% Thus, it seems reasonable to suggest that the accumulation of C_β may contribute to the decrease in catalyst activity

The reaction sequence outlined in Fig 16 is qualitatively consistent with the changes in the surface concentrations of C_α and C_β observed during the course of an experiment Upon introduction of the reaction mixture, the catalyst surface is immediately covered by chemisorbed CO, thereby initiating the deposition of C_α

In the second stage of an experiment, the $^{13}C^{16}O$ present in the reactor bed is replaced by $^{12}C^{16}O$ Since the change in isotopic composition is made without altering the partial pressures of CO and D_2, the surface concentrations of adsorbed CO, carbon, and deuterium are unaffected The rapid displacement of adsorbed $^{13}C^{16}O$ by $^{12}C^{16}O$ means that within the first few seconds following the perturbation in isotopic composition of CO, the source of ^{13}C-labeled C_α and C_β is eliminated The subsequent decline in the surface concentrations of $^{13}C_\alpha$ and $^{13}C_\beta$ is dictated by the kinetics governing the interconversion of these species and the hydrogenation of both forms of carbon to $^{13}CD_4$ The data presented in Figs 9 and 10 show that at the outset, C_α reacts much more rapidly than C_β, even though the reservoir of C_α is about an order of magnitude smaller than that of $^{13}C_\beta$ This indicates that the rate coefficient for conversion of C_α to CD_x is significantly larger than that for C_β With increasing time, the inventory of C_α decreases to the point where C_α is no longer the dominant source of $^{13}CD_4$ and now C_β becomes the principal source of this product

The final phase of an experiment involves the removal of all residual carbon-containing species with D_2 Figure 5 shows that during this phase, the surface concentration of adsorbed CO gradually decreases It is reasonable to postulate that the Ru sites vacated by this means are rapidly covered by adsorbed D_2, and hence that the surface concentration of D_2 increases at a rate comparable to the rate at which adsorbed CO is consumed The reaction sequence presented in Fig 16 indicates that under such circumstances the rate of CD_4 formation will go through a maximum as each of the forms of adsorbed carbon is consumed Since C_α is more reactive than C_β, the peak in CD_4 formation associated with the consumption of C_α will occur earlier than that associated with the consumption of C_β The shift in the position of the peak for C_β to earlier times with increasing reaction temperature, observed in Fig 13, can be attributed to the fact that the global activation energy for converting C_β to CD_4 is higher than that for C_α

CONCLUSIONS

Transient response, isotopic tracer experiments have revealed that two distinctly different forms of carbon are deposited on the surface of a Ru/SiO_2 catalyst during CO hydrogenation The first of these, designated C_α, rapidly achieves a steady-state

coverage This form of carbon is highly reactive and is the principal precursor to methane and C_2^+ hydrocarbons The rate of methanation is directly proportional to the surface coverage by C_α The second form of carbon, designated C_β, accumulates progressively with time, and after a few minutes under reaction conditions, the quantity of C_β on the catalyst exceeds by many fold the quantity of C_α The location of C_β is not fully established It appears that only a part of the total C_β deposit resides on the surface of Ru and that the balance is on the support There is also evidence that the portion on the metal surface may be responsible for the progressive loss of methanation activity with time

The formation of C_α occurs via the dissociation of adsorbed CO, and takes place without the participation of hydrogen C_β, on the other hand, is formed from C_α, and the conversion of C_α to C_β requires the presence of hydrogen on the catalyst surface Quite surprisingly, it is found that C_β can be converted back to C_α Based on these observations, it is concluded that under reaction conditions C_β acts as a reservoir of carbon that can resupply the inventory of C_α

In situ infrared spectra of the catalyst indicate that for the range of reaction conditions considered here, the surface of Ru is virtually saturated by linearly adsorbed CO Less than monolayer coverages of CO could be obtained by a partial reduction adsorbed CO Correlation of the integrated band intensity with the coverage by adsorbed CO has shown that the integrated absorption coefficient, $\bar{A}_{CO}$, is not constant but instead decreases progressively with increasing coverage

ACKNOWLEDGMENTS

This work was supported by the Division of Chemical Sciences, Office of Basic Energy Sciences, U S Department of Energy under Contract DE-AC03-76SF00098

REFERENCES

1 Matsumoto, H , and Bennett, C O , *J Catal* **53,** 331 (1978)
2 Reymond, J P , Mériaudau, P , Pommier, B , and Bennett, C O , *J Catal* **64,** 163 (1980)
3 Ekerdt, J G and Bell, A T , *J Catal* **58,** 170 (1979)
4 Biloen, P , Helle, J N , and Sachtler, W M H , *J Catal* **58,** 95 (1979)
5 Cant, N W , and Bell, A T , *J Catal* **73,** 257 (1982)
6 Kobori, Y , Yamasaki, H , Naito, S , Onishi, T , and Tamaru, K , *J Chem Soc Trans 1* **78,** 1473 (1982)
7 Yamasaki, H , Kobori, Y , Naito, S , Onishi, T , and Tamaru, K , *J Chem Soc Trans 1* **77,** 2913 (1981)
8 Biloen, P , Helle, J N , van den Berg, F G A , and Sachtler, W M H , *J Catal* **81,** 450 (1983)
9 Happel, J , Suzuki, I , Kokayeff, P , and Fthenakis, V , *J Catal* **65,** 59 (1980)
10 Happel, J , Cheh, H , Otarod, M , Ozawa, S , Severidia, A J , Yoshida, T , and Fthenakis, V , *J Catal* **75,** 314 (1982)
11 Otarod, M , Ozawa, S , Yiu, F , Chew, M , Cheh, H Y , and Happel, J , *J Catal* **71,** 216 (1981)
12 Hicks, R F , Kellner, C S , Savatsky, B J , Hecker, W C , and Bell, A T , *J Catal* **71,** 216 (1981)
13 Savatsky, B J , and Bell, A T , *ACS Symp Ser* **178,** 105 (1982)
14 Kellner, C S , and Bell, A T , *J Catal* **70,** 418 (1981)
15 Kellner, C S , and Bell, A T , *J Catal* **71,** 288 (1981)
16 Vannice, M A , *J Catal* **58,** 170 (1979)
17 Dalla Betta, R A , Piken, A G , and Shelef, M , *J Catal* **35,** 54 (1974)
18 Hammaker, R M , Francis, S A , and Eischens, R P , *Spectrochim Acta* **21,** 1295 (1965)
19 Heyne, H , and Tompkins, F C , *Trans Farad Soc* **63,** 1274 (1967)
20 Eischens, R P , *Acc Chem Res* **5,** 74 (1972)
21 Seanor, D A , and Amberg, C H , *J Chem Phys* **42,** 2967 (1965)
22 Cant, N W , and Donaldson, R A , *J Catal* **78,** 461 (1982)
23 Pfnur, H , Menzel, D , Hoffman, F M , Ortega, A , and Bradshaw, A M , *Surf Sci* **93,** 431 (1980)
24 Crossley, A , and King, D A , *Surf Sci* **68,** 528 (1977)
25 Crossley, A , and King, D A , *Surf Sci* **95,** 131 (1980)
26 Duncan, T M , Winslow, P , and Bell, A T , *Phys Chem Lett* , in press
27 Bell, A T , *Catal Rev Sci Eng* **23,** 203 (1981)
28 Biloen, P , and Sachtler, W M H , "Advances in Catalysis," Vol 30, p 165 Academic Press, New York, 1981
29 Goodman, D W , Kelley, R D , Madey, T E , and White, J M , *J Catal* **64,** 479 (1980)